EUROPEAN ORGANIZATION FOR NUCLEAR RESEARCH

CERN SL/98-029 (AP)

# BEAM DYNAMICS AT LEP

**John M. Jowett**

**Abstract**

LEP has proved to be one of the most flexible $e^+e^-$ colliders built to date. It has operated at various energies, in several modes, with ever-increasing demands for luminosity in clean and precisely known beam conditions. Together with some unique features, LEP therefore has much in common with future $e^+e^-$ factories. Beam-dynamical phenomena have been among the crucial determinants of LEP's performance. These include single-particle dynamics (optics design, dynamic aperture, radiation effects, etc.), a variety of beam-beam effects and collective instabilities. The strategies adopted to overcome these effects and maximise performance will be described with emphasis on those relevant to the design and operation of $e^+e^-$ factories.

*Invited talk at the Advanced ICFA Beam Dynamics Workshop on "Beam Dynamics Issues for $e^+e^-$ Factories", Frascati, 20-25 October 1997*

Geneva, Switzerland

June 23, 1998

# Contents


**1 Introduction** **3**
1.1 LEP and the (other) factories . . . . . 3

**2 General Description of LEP** **4**
2.1 Global Parameters . . . . . 4
2.2 Cycle of Operation . . . . . 4
2.3 LEP layout and optics . . . . . 5

**3 LEP1** **6**
3.1 Beam parameter variation and control . . . . . 6
3.2 Beam-beam effects and luminosity . . . . . 8
3.3 Intensity Limits from Beam Dynamics . . . . . 9
3.3.1 Increasing Intensity . . . . . 10

**4 Multi-bunch schemes** **12**
4.1 Local Vertical Separation Bumps . . . . . 12
4.2 Pretzel scheme, Z-factory . . . . . 12
4.2.1 Optical side-effects and their correction . . . . . 14
4.2.2 Beam-beam effects and intensity limit . . . . . 15
4.2.3 Pretzel Intensity Limit . . . . . 15
4.2.4 Achieving performance . . . . . 16
4.3 Bunch Train Scheme . . . . . 16
4.3.1 Side effects . . . . . 17
4.3.2 Monochromatization and collision energy shift . . . . . 18
4.4 General remarks on multi-bunch schemes . . . . . 18

**5 LEP2** **19**
5.1 Attaining high luminosity . . . . . 19
5.2 Vertical beam size . . . . . 20
5.3 Single particle dynamics with radiation . . . . . 20
5.4 Nonlinear Dynamics and Dynamic Aperture . . . . . 24

**6 Conclusions** **27**

# 1 Introduction

LEP started operation in 1989. However the matter subsumed by the title of this talk is vast and diverse and has been under study now for over 20 years. The only way to keep within my time is to cleave to a pretty narrow definition of Beam Dynamics and focus on those issues that are either: *relevant to new* $\mathrm{e^+e^-}$ *factories*, or *unique to LEP*. I shall tend to omit, or mention only in passing, the important but well-understood topics in beam dynamics that LEP has in common with other colliders. More unreasonably, I will not discuss the spin polarization and energy calibration. You will hear little mention of hardware—even such monumental achievements as the super-conducting (or indeed the normal-conducting...) accelerating system—in this talk. The same goes for operational aspects, instrumentation, diagnostics and so forth. A few of these omissions will be made good by speakers in the working groups and, fortunately, there is ample review and specialised literature for the rest.

## 1.1 LEP and the (other) factories

LEP is often seen as the end of a line of "classical" $\mathrm{e^+e^-}$ colliders, starting with machines like ADONE, here in Frascati, and evolving through the likes of SPEAR, VEPP-4, PETRA and TRISTAN. The main thread of this evolution has been steadily increasing energy (and size). Otherwise, most of these machines operated with a small number of bunches (close to the number of interaction regions) and broadly similar design principles that can be summed-up in the familiar formulas. The baseline design of LEP was the extrapolation of these principles to about the largest economically feasible energy (in anticipation, more or less, of the development of super-conducting RF).

During the 1980s, however, the design principles of $\mathrm{e^+e^-}$ colliders underwent some mutations, expressed notably in the continual upgrading of CESR to reach higher luminosity. These ideas culminated in the *factory* concept that we are here to work on. In my opinion, LEP has shared in these evolutionary offshoots. A look at the cross-section for $\mathrm{e^+e^-}$ annihilation [1] makes it obvious why it should: LEP initially operated in a high-luminosity mode ("LEP1") for high-precision physics at the energy of a specific resonance—the Z boson—just as the new factories are designed to do (note that this energy was not well known when the baseline design was specified). This design was indeed modified to increase the number of bunches and considerable effort was put into calibrating the beam energy with the necessary precision. These features are less in evidence for the present "LEP2" operation above the W-pair threshold where the energy is determined by the accelerating voltage available.

| | | | |
|---|---|---|---|
| Circumference | $C$ | 26658.9 | m |
| No. of IPs | | 4 | |
| No. of straight sections | | 8 | |
| Momentum compaction* | $\alpha_c$ | $1.85 \times 10^{-4}$ | |
| Tunes* | $Q_x$ | 90.26 | |
| | $Q_y$ | 76.19 | |
| Mean bend radius | $\rho_0$ | 3026 | m |
| Variation of damping partition number* | $\frac{dJ_\epsilon}{d\delta}$ | 315 | |

Table 1: Some energy-independent parameters for LEP. All wigglers are taken to be switched off. Those parameters marked "*" refer to the $(90^\circ, 60^\circ)$ optics (see Section 2.3 below).

# 2 General Description of LEP

## 2.1 Global Parameters

Parameter lists are hostages to fortune for accelerator designers. This is particularly so in the case of LEP where the operating conditions have changed so much. Table 1 lists a rather few global parameters of LEP that are valid in most conditions.[1]

## 2.2 Cycle of Operation

Unlike the lower-energy factories, LEP does not have a full-energy injector. Injection takes place at 22 (formerly 20) GeV with beams separated electrostatically at all encounter points. Injection can be into either betatron or synchrotron phase space. In synchrotron phase space injection [2], the particles of the injected pulse have a momentum deviation $\Delta p = D_x x_{\rm inj}$ where $D_x$ and $x_{\rm inj}$ are the dispersion and injection offset. Thus they find themselves immediately executing synchtron oscillations rather than betatron oscillations around the closed orbit. Synchrotron injection has been found most favourable in recent years, particularly as it can allow two injector bunches to fill a single LEP bunch within one basic cycle [3].

When sufficient beam current is accumulated the machine is ramped to a collision energy. This is currently 91.5 GeV, but has been $45.6 \pm 2\,\mathrm{GeV}$, 65–68, 80.5, 86 ... GeV. Before allowing the beams to collide at the 4 interaction points, the orbit, tunes and other quantities are corrected, the optical functions at the interaction points are "squeezed" to their "physics" values (usually $\beta_y^* = 0.05\,\mathrm{m}$), the beam size may be adjusted, etc. Once good conditions, including acceptably low backgrounds, are achieved, the experiments start to take data. During this time (the "coast"[2]) the operators continue to adjust as necessary (see Section 3.2). When, after several hours,

[1] Tables 1 and 2 also serve to define notations.

[2] For want of a better word... of course, beams in LEP never coast for long in the usual sense!

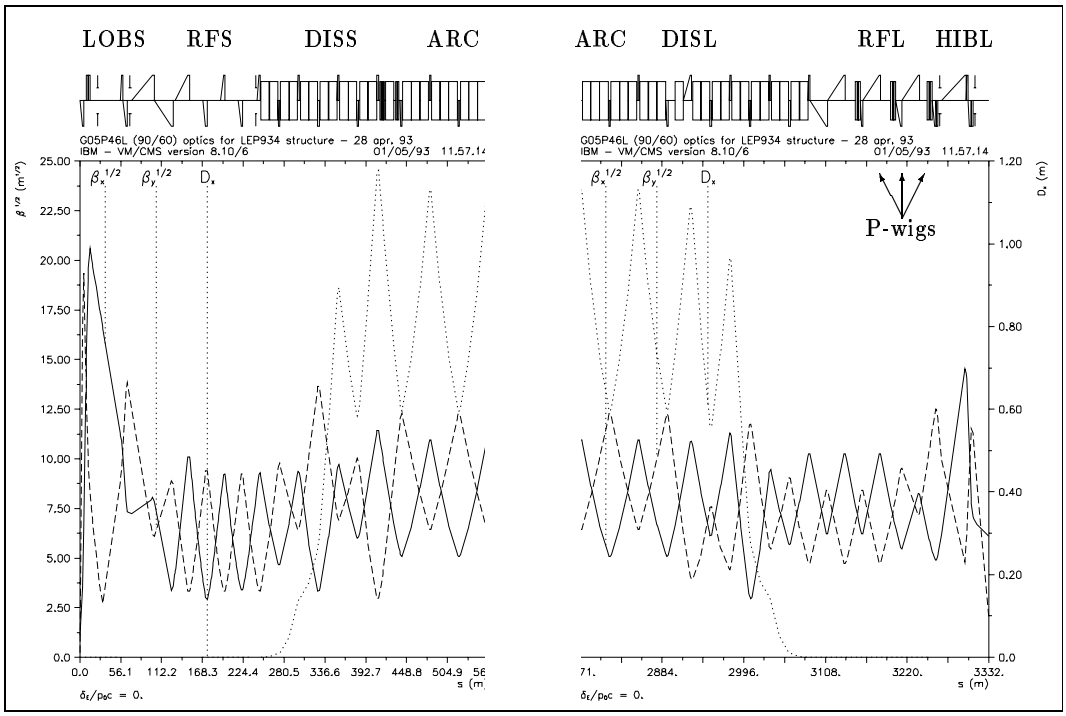


Figure 1: A typical LEP optics in one octant (IP2 to IP3) of the ring. On the left is an "even" numbered interaction point and experimental insertion consisting of a low-$\beta$ insertion (LOBS), RF section (RFS) and dispersion suppressor (DISS). On the right, the "odd" non-experimental insertion consists of a dispersion suppressor (DISL), unused RF section (RFL) and "high-$\beta$" insertion (HIBL) with higher values of $\beta_{x,y}$ than at the even point. Most of the long chain of 31 FODO cells in the arc is suppressed. Three "polarization" wigglers are visible in the RFL insertion.

intensity and luminosity have decayed, they dump the beams and recycle the machine.

### 2.3 LEP layout and optics

Figure 1 shows the optics of one octant. Roughly speaking, the full ring is constructed by reflecting about either end and repeating 4 times. In reality, the resulting symmetry is broken in many details. The normal-conducting RF system, providing some 350 MV was installed on either side of IP2 and IP4. The super-conducting RF for LEP2 is installed around all even interaction points.

LEP1 started up with phase advances in the arc cells of $(\mu_x, \mu_y) = (60°, 60°)$ with $(90°, 90°)$ seen as an alternative for lower single bunch currents and higher energy. Indeed a $(90°, 90°)$ optics was run at Z-energy in 1992. Since 1993, however, most operation has been with a $(90°, 60°)$ optics. The change in $\mu_y$ was motivated largely by its suitability for polarization of the beams. Other, more exotic, phase advances

have been tried and are foreseen for the highest energies.

LEP is flexible enough to accommodate these and many other optical changes thanks to the modular structure of the lattice [4, 5].

The experiments are located at the even-numbered interaction points (2,4,6,8) while local electrostatic vertical separation avoids head-on beam-beam encounters at the odd points (1,3,5,7). For a $(90°, 60°)$ optics, chromaticity is corrected with 2 sextupole families (SF) in the horizontal plane and 3 families (SD) in the vertical. The families are *interleaved*:

```
octant=(IP2,SD1,SF2,SD2,SF2,SD3,SF1,SD1,SF2, ...
        ....,SF1,SD3,SF2,SD1,SF1,SD2,IP3)
```

To switch to an optics with $\mu_y = 90°$, it is necessary to manually recable the SDs into two families for adequate chromaticity correction. Although something of an impediment to frequent changes of optics, this was first done for the 1992 run and has been done again a few times since.

# 3 LEP1

The initial period of operation from 1989-95 at the Z-resonance (and nearby scan points 44.72, 46.51...GeV) is referred to as LEP1. A set of parameters typical of good conditions is given in Table 2.

## 3.1 Beam parameter variation and control

The fractional energy spread is given by the well-known formula

$$\sigma_\varepsilon^2 = \left\langle \varepsilon^2 \right\rangle = \left\langle \left( \frac{E - E_0}{E_0} \right)^2 \right\rangle = \frac{55}{32\sqrt{3}} \frac{\hbar}{m_e c} \left( \frac{E_0}{m_e c^2} \right) F_\varepsilon, \quad \text{where} \quad F_\varepsilon = \frac{\int |G(s)|^3 \, ds}{J_\epsilon \int G(s)^2 \, ds} \tag{1}$$

where $G(s) = eB_y(x_c, y_c, s)/p_0 c$ is the local bending strength on the closed orbit. In an idealised isomagnetic ring[3] , $B_y(s) = B_0 = \text{const.}$, $F_\varepsilon \approx 2\pi/\rho_0 \propto B_0/E$. However wiggler magnets with $B \gg B_0$ can substantially modify $F_\varepsilon$ and so modify the natural dependence $\sigma_\varepsilon \propto E_0$.

Similarly the horizontal emittance

$$\epsilon_x = \frac{55}{32\sqrt{3}} \frac{\hbar}{m_e c} \left( \frac{E}{m_e c^2} \right) F_x, \qquad \text{where} \qquad F_x = \frac{\int \mathcal{H}(s) |G(s)|^3 \, ds}{J_x \int G(s)^2 \, ds} \tag{2}$$

can be increased by wigglers at dispersive locations ($\mathcal{H} > 0$).

LEP has some 20 strong wigglers [6, 7] and they play a vital role in maximising performance. Each has a strong centre-pole field, $B_+$, and weaker outer poles:

[3]This common approximation also assumes that the design closed orbit passes through the centres of the quadrupoles. This is far from true at LEP—see later.

| | | | |
|---|---|---|---|
| Beam energy | $E$ | 45.6 | GeV |
| No. of bunches | $k_b$ | 8 | |
| Damping partition | $J_x$ | 1 | |
| | $J_y$ | 1 | |
| | $J_\epsilon$ | 2 | |
| Main bend field | $B_0$ | 0.05 | T |
| Field in emittance wigglers | $B_{\rm EW}$ | 0.85 | T |
| Critical energy of syn. radn. | $u_c$ | 69.5 | keV |
| Photon emission rate | $N/c$ | 0.31 | photons/m |
| Energy loss/turn | $U_0$ | 134.28 | MeV |
| Radial damping time | $\tau_x$ | 0.06 | s |
| | $\tau_x/T_0$ | 679 | turns |
| Energy spread | $\sigma_\varepsilon$ | $0.946 \times$ 10-3 | |
| Emittances (no beam-beam) | $\epsilon_x$ | 22.5 | nm |
| | $\epsilon_y$ | 0.29 | nm |
| Particles/bunch | $N_b$ | $1.66 \times 10^{11}$ | |
| Single bunch current | $I_b$ | 0.3 | mA |
| Twiss functions at interaction point | $\beta_x^*, \beta_y^*$ | 2.0, 0.05 | m |
| Beam sizes at interaction point | $\sigma_x^*, \sigma_y^*$ | 211, 3.8 | $\mu$m |
| Radiated power (2 beams) | $P_{\rm rad}$ | 0.645 | MW |
| Beam-beam parameters | $\xi_x, \xi_y$ | 0.037, 0.042 | |
| Luminosity | $L$ | $2 \times 10^{31}$ | $\rm cm^{-2}s^{-1}$ |
| Peak RF voltage | $V_{\rm RF}$ | 380 | MV |
| Synchrotron tune | $Q_s$ | 0.085 | |
| Bunch length (low current) | $\sigma_z$ | 0.877 | cm |
| Beam-beam lifetime | $\tau_b b$ | 18 | h |

Table 2: Parameters for LEP1 operation at the Z resonance, typical of good conditions with the pretzel scheme in 1994.

**4 "damping" wigglers** ($B_+ = 1.1\,\mathrm{T}$) in dispersion-free locations serve to increase damping *and* lengthen bunches at injection;

**4 "emittance" wigglers** ($B_+ = 1.1\,\mathrm{T}$) at dispersive locations have the same effects but also increase $\epsilon_x$ in physics conditions;

**12 "polarization" wigglers** ($B_+ = 1.3\,\mathrm{T}$) are stronger damping wigglers. These were added later and are more difficult to operate as they require a tricky compensation of residual orbit effects.

It is only feasible to use wigglers like these as transparent beam-parameter controls if corrections of their tune-shifts, $\Delta Q_y \propto B_+^2/E^2$ (by rematching of nearby quadrupoles) are programmed into their "knobs". These also include non-linear excitation of trim coils and nearby orbit correctors to ensure zero net orbit displacement. Thus

"switching on the wigglers" is a fairly complicated operation with compensations that vary in a complicated fashion during energy ramping.

Variation of damping partition numbers $J_\epsilon$ and $J_x \simeq 3 - J_\epsilon$ provides an additional degree of freedom in control of (1) and (2). This is achieved by a small change of the RF frequency that changes the momentum on the closed orbit and in turn changes [8]

$$\begin{aligned} J_\epsilon(\delta) &= \frac{d\,\log U(\delta)}{d\delta} \approx 2 + \left[\frac{2\int K_1^2(s) D_x^2(s)\,ds}{\int G^2(s)\,ds}\right]\delta \\ &\approx 2 + 4\left(\frac{L_{\rm bend}}{L_{\rm quad}}\right)\frac{2+\frac{1}{2}\left(\sin\frac{\mu_x}{2}\right)^2}{\left(\sin\frac{\mu_x}{2}\right)^2}\delta \qquad \text{(thin lens FODO, no wigglers)} \end{aligned} \tag{3}$$

To be more precise, the momentum of a general particle [8] at azimuth $s$ is $p = p_0(1 + \delta(s) + \varepsilon)$ and

$$\langle\delta(s)\rangle = -\frac{1}{\alpha_c}\frac{\Delta f_{\rm RF}}{f_{\rm RF}} \tag{4}$$

is the shift of the *average beam momentum on the closed orbit* from its central value. I stress this since, in LEP, the notion of a constant momentum closed orbit is very far from the physical reality (as is the notion of "dispersion" deriving from "off-momentum closed orbits"). The additional component $\varepsilon$ is the canonical momentum variable for synchrotron oscillations.

Wigglers always increase $\sigma_\varepsilon$ and the total amount of radiation damping. Manipulating $J_\epsilon$ allows $\sigma_\varepsilon$ to be reduced at the price of reduced transverse damping and larger $\epsilon_x$. However, because of the great importance of precisely calibrating the collision energy, variations of $J_\epsilon$ were not allowed during operation at the Z. This was one knob for increasing luminosity that we had to forgo. It has become possible to exploit it in physics only this year, at LEP2 energies.

### 3.2 Beam-beam effects and luminosity

The luminosity of a collider like LEP is given by

$$L = \frac{k_b f_0 N_+ N_-}{4\pi\sigma_x^*\sigma_y^*} \tag{5}$$

where $f_0 = c/C$ and I shall assume equal bunch populations $N_+ = N_- = N_b$ in the following. Introducing the usual beam-beam strength parameters

$$\xi_x = \frac{N_b r_e \beta_x^*}{2\pi\gamma(\sigma_x^* + \sigma_y^*)\sigma_x^*}, \qquad \xi_y = \frac{N_b r_e \beta_y^*}{2\pi\gamma(\sigma_x^* + \sigma_y^*)\sigma_y^*} = \frac{\beta_y^*\sigma_x^*}{\beta_x^*\sigma_y^*}\xi_x \tag{6}$$

so that the bunch current is determined by

$$I_b = eN_b f_0 = \frac{2\pi e f_0 \gamma \epsilon_x \xi_y}{r_e(1+r)}, \qquad r = \frac{\sigma_y^*}{\sigma_x^*} \tag{7}$$

and (5) can be rewritten as

$$L = \frac{\pi k_b f_0 (1+r)^2 \gamma \epsilon_x \xi_y^2}{r_e \beta_y^*} = \frac{\gamma I_b}{2 e r_e} \frac{\xi_y}{\beta_y^*}(1+r) \approx 2.17 \times 10^{32} (1+r) \xi_y \frac{[I/\mathrm{mA}][E/\mathrm{GeV}]}{[\beta_y^*/\mathrm{m}]} \tag{8}$$

LEP has had beam-beam blow-up in both planes. The usual vertical blow-up is seen for large $\xi_y$ (see (6)) but horizontal blow-up also occurred at LEP1 when $\xi_x$ became too large. As foreseen in the original design, the four emittance wigglers were used at the start of "coasts" to reduce $\xi_y$, avoiding flip-flop effects, poor lifetime, etc. As the intensity decayed, they could be turned down in order to stay close to the beam-beam limit and thus maximise integrated luminosity.

The bunch currents that could be collided at 45.6 GeV were limited by backgrounds. It was impossible to collimate adequately for $\epsilon_x \gtrsim 45\,\mathrm{nm}$. This, not collective effects at injection, was the limit on bunch current, $I_b \lesssim 0.35\,\mathrm{mA}$, at LEP1.

Coherent beam-beam oscillations were occasionally observed but were usually damped by chromaticity and did not affect performance.

A so-called "golden orbit" is an vital ingredient for good beam-beam performance [9]. It has the essential characterisitic of passing through the centres of the interaction region quadrupoles and minimising dispersion at the interaction points.

These topics will be discussed further in the working groups [10, 11].

### 3.3 Intensity Limits from Beam Dynamics

Single-beam collective instabilities usually loom large in every collider's design study and programme of machine experiments; LEP is no exception to this rule. It comes therefore as a bit of a surprise that beam intensities (collided for physics) in LEP have (so far) rarely been limited by beam-dynamical effects. Even the present (LEP2) intensity limits arise from losses in super-conducting cavities and heating of vacuum elements. Nevertheless, as we confidently expect the blame to be shifted back to beam dynamics before long, it is worth summarising the main points here. A number of published papers treat these topics in greater depth [12, 13]. Good agreement has been established between computations and measurements of the longitudinal and transverse impedances. Elegant experiments have even localised the sources of impedance around the ring [14].

*Coupled-bunch instabilities* are not very important and were efficiently cured by longitudinal feedback very early on.

A clear *bunch-lengthening* as a function of bunch current has been measured and the threshold has provided good estimates of the longitudinal impedance. In normal operation the turbulent bunch-lengthening does not occur as we lengthen the bunches in a controlled fashion with wigglers, manifestly a better thing to do.

*Synchro-betatron resonances*, both the coherent and incoherent sorts, are clearly seen. The main driving mechanism is coupling ("dispersion") in the RF cavities [15].

It is important to avoid these by avoiding unfavourable changes of betatron and synchrotron tunes during the energy ramp.

*Robinson instabilities* are a feature of a ring containing so many high-Q superconducting cavities.

The *transverse mode-coupling instability (TMCI)* has always been expected to be the ultimate limit on single-bunch current. The threshold bunch current for this instability is, roughly [12],

$$I_b = \frac{2\pi Q_s E}{e \sum_i \beta_i k_\perp(\sigma_z)} \tag{9}$$

The related head-tail modes have been frequently seen, with occasional spectacular 3D viewing on the streak camera. Attempts to counter this instability by means of a special transverse feedback system have not so far been successful.

A detailed model of the transverse impedance has been derived from growth rates and frequency shifts. TMCI occurs at $I_b = 600\,\mu$A for a bunch length $\sigma_z = 2\,\mathrm{cm}$ ($(90°, 60°)$ optics with wigglers at 20 GeV) or at $I_b = 750\,\mu$A for $\sigma_z = 3\,\mathrm{cm}$ ($(60°, 60°)$ optics with wigglers at 20 GeV). Here again there is very good correspondence between theory and measurements. In future a strategy of increasing the synchrotron tune $Q_s$ will be used to push the threshold as high as possible.

The single-beam TMCI threshold is modified by long-range beam-beam effects (Section 4.2.3) when there are two beams in the ring.

### 3.3.1 Increasing Intensity

Understanding the intensity limits, particularly those embodied in (9), has suggested a number of ways to increase the beam intensity. Among these are:

**Remove impedance:** since the normal-conducting RF cavities are the dominant contribution to $Z_\perp$ some are being removed, now that their accelerating voltage can be made up with the super-conducting cavities. Beyond a certain point the gain is slower since the bellows connecting the vacuum chambers are a comparable source of $Z_\perp$.

**Lengthen bunches:** The transition to a more strongly-focused optics ($\mu_x = 60° \rightarrow 90°$ actually shortened the bunches (see Figure 2). The situation was saved by commissioning the "polarization" wigglers which substantially increased the bunch length and the radiation damping rate.

Lengthening bunches by reducing the longitudinal damping (increasing $J_x$) is less favourable and has not been used at injection.

**Higher synchrotron tune** although it may complicate energy ramp (avoidance of synchro-betatron resonances).

**Higher injection energy:** $I_b$ indeed increased by 10% when it was raised from 20 to 22 GeV.

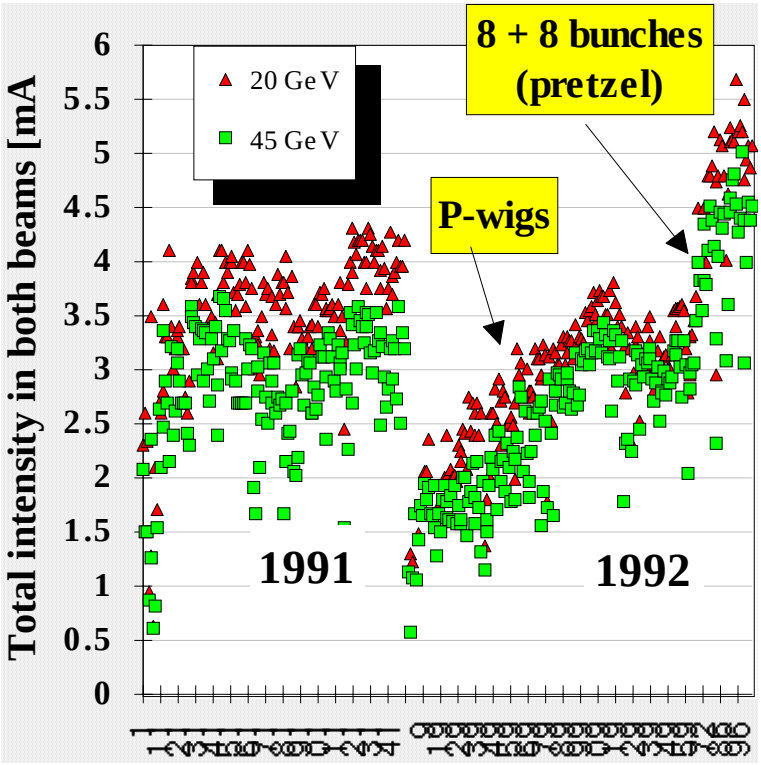


Figure 2: Major steps in beam intensity at LEP: evolution of the intensities at 20 and 45 GeV between 1991 and 1992.

**Reduce $\beta$-functions at impedance sources:** the sensitivity of the beam to wake-fields generated in the RF cavities was minimised in the original design of the optics. Increasing $\mu_y$ from $60^\circ$ to $90^\circ$ reduces $\beta_y$ at the bellows and appears to increase the storable current.

**Increase the number of bunches:** increasing the number of bunches from the original 4 to 8 brought a substantial increase in the total intensity (see Figure 2 and Section 4).

# 4 Multi-bunch schemes

Since $k_b$ bunches per beam collide in $2k_b$ encounter points around the ring, any $k_b > 2$ in LEP creates unwanted encounters beyond those in the four experiments. The resulting beam-beam effects have to be avoided by separating the closed orbits of the two beams at these encounters. Three different electrostatic separation schemes have been used to increase the number of bunches in LEP.

## 4.1 Local Vertical Separation Bumps

The initial design of LEP [5] included local electrostatic bumps to separate the bunches at the odd interaction points (e.g. on the right in Figure 1) and allow $k_b = 4$ evenly-spaced bunches per beam. Similar bumps are used at the experimental interaction points to separate the beams during injection and ramping. This scheme has been used successfully since the beginning of LEP operation. Fine-adjustment of the separation at the interaction points is essential for eliminating small residual separations that can arise from various effects.

It is worth noting that, as with most separation schemes, the *total* beam current that can be stored does not quite increase proportionally to $k_b$ [16]. Residual beam-beam effects influence the "single-bunch" instabilities.

A scheme for vertical separation in the middles of the arcs to allow $k_b = 8$ was considered early on [17] but never implemented, mainly for reasons of cost. This would have been the limit on $k_b$ compatible with the power-saving system of storage cavities attached to the initial normal-conducting RF system.

## 4.2 Pretzel scheme, Z-factory

The success of the pretzel scheme in CESR [18] inspired a suggestion [19] to try the same thing in LEP. It was seen as a means of exploiting the large LEP2 installation of RF power at LEP1 energy. The LEP pretzel scheme [20, 21] was conceived as a "Z-factory" upgrade programme for a LEP with a purely super-conducting RF system. By means of horizontal separation everywhere except in the experimental straight sections, it would have allowed $k_b = 2$, 4, 6, 8, 10, 12, 18, 24, or 36 evenly-spaced bunches per beam without close beam-beam encounters.

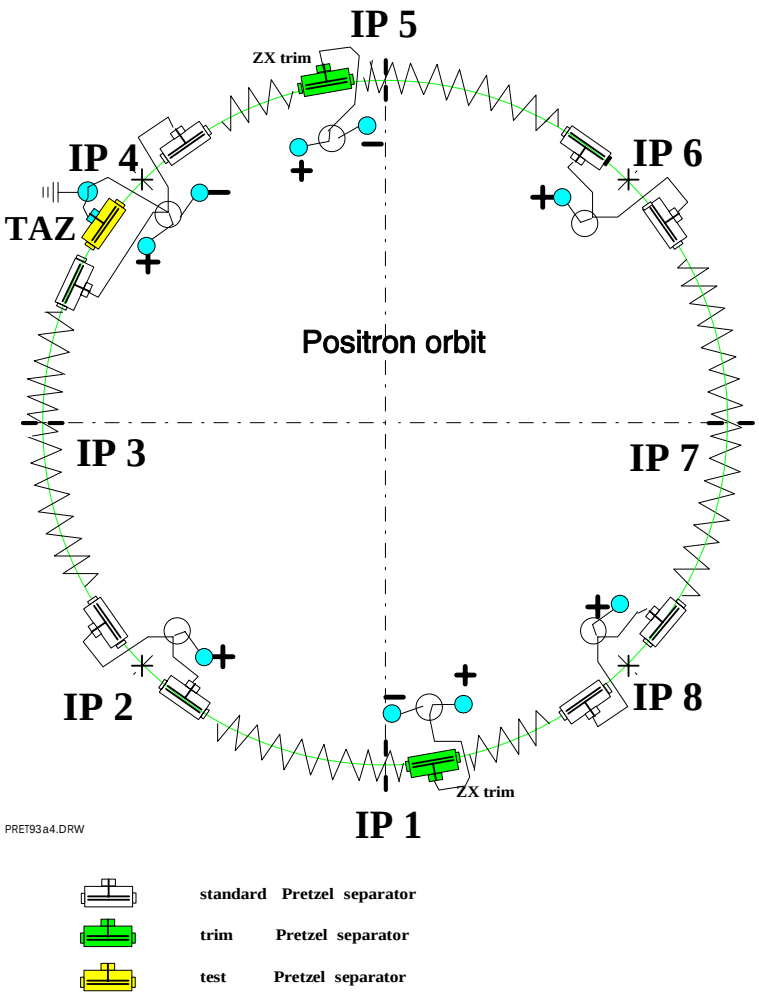


Figure 3: Pretzel scheme for 1993 including trim separators at IP1 and IP5, showing the scheme for exciting the separators and a positron orbit. (The “TAZ” test separator was not used in the operational pretzel scheme.)

When some electrostatic separators became available from the de-commiss ioning of the SPS as a $\mathrm{p\bar{p}}$ collider, we seized the chance to implement a "Crash" version of the pretzel scheme(Figure 3). It was limited to $k_b = 8$ because of the normal-conducting RF and the need to avoid immediate upgrades of the detectors. LEP ran in pretzel mode for parts of the 1992 and 1993 runs and all of 1994's.

### 4.2.1 Optical side-effects and their correction

Since the orbits of electrons and positrons are separated by several mm, the two beams experience different magnetic fields and their optical functions and parameters can be significantly different. The most immediately obervable effects of separated orbits (and their interaction with the RF voltage distribution) was a vertical tune-split $|Q_y^+ - Q_y^-| \simeq 0.02$. Correction was achieved by installing special sextupoles in straight sections where the orbits were separated but the dispersion was small.

Phase-advance differences between the beams also complicated the correction of the pretzel closure. Out of a variety of measurement methods, analysis of the multi-turn data from the orbit measurement system proved most effective in establishing the condition of $\mu_x = 42\pi$ between the centres of the pretzel separators. The correction was achieved by adjusting horizontal phase advance "trombones" composed of 6 quadrupole families in each quadrant. The tunes of the ring were kept constant by compensating trims in the experimental insertion.

Errors in the machine also led to residual horizontal separations of the beams at the interaction points. However local separators were only available for the vertical plane and, as Figure 3 shows, the pretzel separators for adjacent quadrants had to share high-voltage supplies. So the 8 main separators all had to have same voltage and there might have been no functional independence between the 4 long pretzel bumps! However, by changing the gaps between the motorised electrodes, their electric fields could be varied independently within a certain range. Together with two additional independent separators at IP1 and IP5, this provided just enough parameters to empirically remove the separations at the 4 interaction points.

However the most important compensation was built into the design of the pretzel scheme from the beginning: *anti-symmetry of the pretzel separation around every interaction point* ensured that, at least in the ideal machine, many of the differential effects between the beams cancelled out from one octant to the next (see Figure 3). Pretzel operation would have been much more difficult, perhaps impossible, without this.

The most intractable side-effects tended to arise from the perturbation of the dispersion function $D_{x0} \to D_x$ when pretzel orbits passed off-centre through sextupoles. Depending on the betatron phase between the pretzel separators and the arc quadrupoles, this effect could be substantial. Among other things, it changed the damping partition (analogously to (3)):

$$J_\epsilon \simeq 2 + \frac{2 \int K_1^2(s)\,(D_x - D_{x0})\,x_p(s)\,ds}{\int G^2(s)\,ds} \tag{10}$$

and led to differences of $J_x$ and the horizontal emittance $\epsilon_x$, (2), between the beams. Given the many other constraints imposed on the phase advances around the ring, it was not possible to eliminate this effect completely. The anti-symmetry did not help because the effect was *second-order* in pretzel amplitude.

The pretzel side-effects gave us a foretaste of those now arising from "energy-sawtoothing" at LEP2 and would have provided ways of counteracting them. It is worth mentioning here that there was good agreement between measurements and calculations of the systematic optical perturbations by pretzels. In practice this was a matter of modelling the machine correctly with the program MAD. Perturbative formulas also work fairly well.

### 4.2.2 BEAM-BEAM EFFECTS AND INTENSITY LIMIT

The pretzel scheme added horizontally separated beam-beam encounters in the middle of each arc to the existing cocktail of head-on collisions at the interaction points and vertically separated encounters at the odd points. These encounters took place in a horizontally focusing quadrupole at a location of maximum $D_x$. The design [20, 21] used conservative semi-empirical criteria such as a minimum scaled separation $N_\sigma = X/\sigma_x$ or maximum values of the parasitic tune-shift parameters $\xi^p_{x,y}$ for sufficient horizontal separation.

We did a few experiments exploring the question of minimum separation necessary in physics conditions. Figure 4 shows an example where the pretzel separator voltage was reduced until the lifetime deteriorated. Variation of $J_x$ was then used to go beyond the limit. There was some unavoidable re-optimisation of conditions during experiment. Initial intensities of $I_b \approx 150\,\mu$A were reduced to $I_b \approx$ 110–130 $\mu$A by the end. The head-on beam beam effects were not very strong ($\xi_y \simeq 0.01$). At first we seemed to find that there was a minimum necessary separation $N_\sigma \simeq 5$. However by adjusting the tunes it was possible to reduce the pretzel separation to zero, through a perilous region around $N_\sigma \simeq 4$, and restore good lifetime.

I quote this example to indicate that counter-examples to most minimum separation criteria can be found; there does not appear to be a simple *necessary* criterion. It was better to have a margin of separation available and to find a practical optimum (usually around $7\sigma_x$) empirically. Too large a separation could increase some of the optical side-effects of the pretzels to unacceptable levels.

### 4.2.3 PRETZEL INTENSITY LIMIT

As mentioned in Section 4.1, parasitic beam-beam effects can combine with single-bunch collective effects to reduce the single-bunch current. In the pretzel scheme these effects were stronger and reduced the attainable $I_b$ to $\simeq 350\,\mu$A. The reduction was mainly due to the enhancement of the horizontal "$m = -1$" head-tail mode by the large $D_x$ at the encounters. A $2 + 2$ particle model and simulation of these effects can be found in [16].

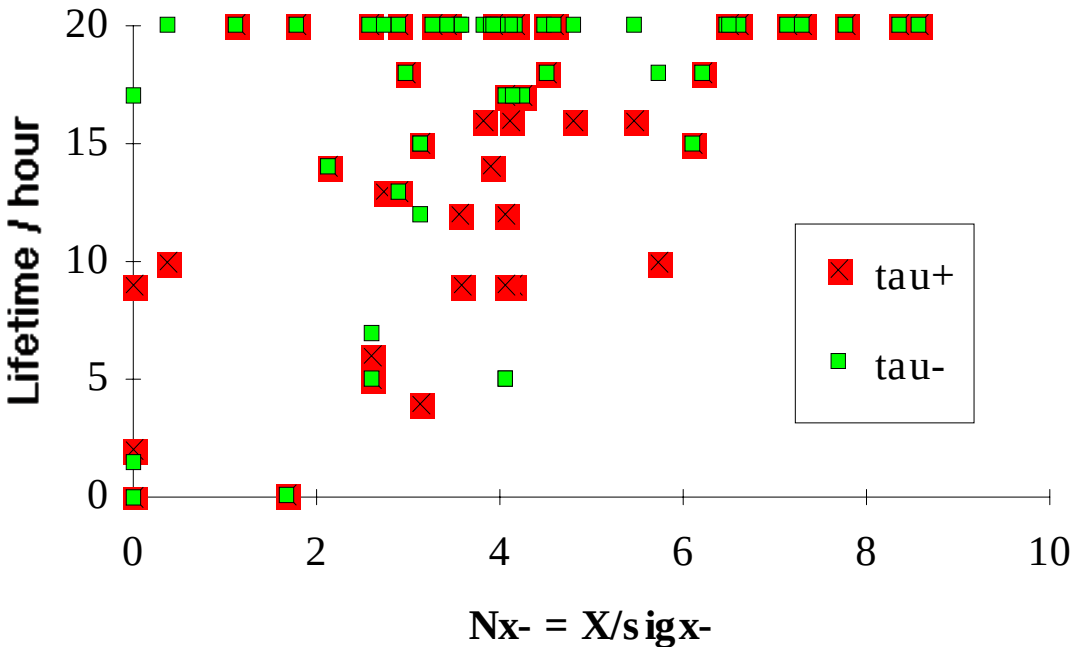


Figure 4: Beam lifetimes as a function of separation, in an experiment with colliding beams at 45.6 GeV, expressed in units of the computed beam size.

Synchrotron phase space injection was introduced in the last experiment [22] carried out in the pretzel configuration. Together with the use of negative chromaticity to stabilise the "$m = -1$" mode and feedback to stabilise the dipole mode, it was possible to overcome this complex instability and again reach the single-beam limit on $I_b$ determined by TMCI.

#### 4.2.4 Achieving performance

At first, the pretzel scheme gave the same luminosity as the preceding 4-bunch operation. Following a learning process to improve machine conditions (particularly the use of "golden" orbits) and compensate the side effects, the luminosity doubled. The 1994 run provided the best harvest of integrated luminosity to date[4].

### 4.3 Bunch Train Scheme

Increasing the number of bunches beyond $k_b = 8$ in the pretzel scheme would have required new investment in the LEP detectors and some modifications to the machine [21]. The proposed bunch train scheme [23] hoped to go further at the price of a lesser investment in the machine. The idea was to group 2, 3 or 4 bunches into

[4]It looks as if 1997 may exceed that but at twice the beam energy.

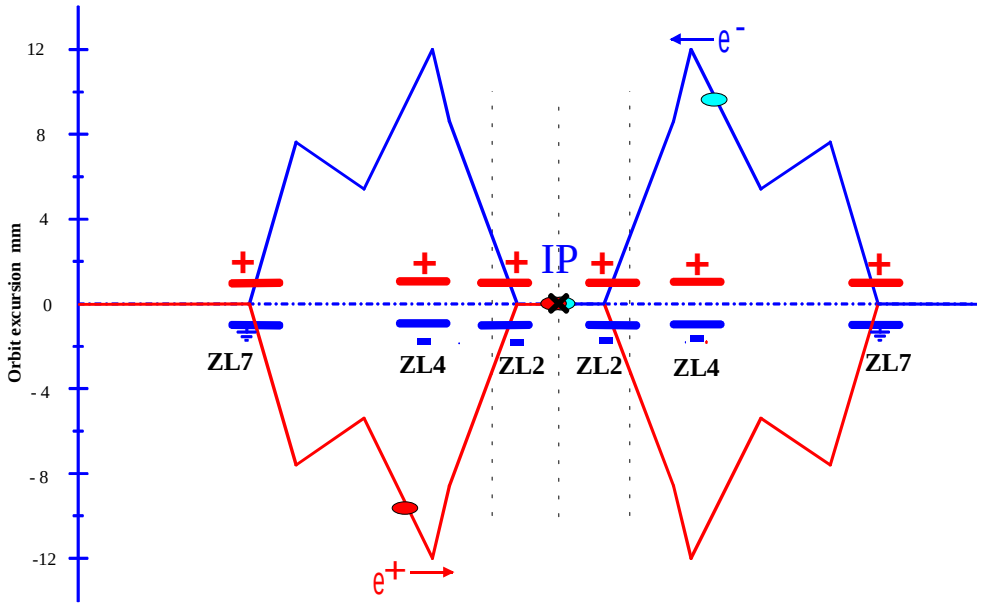


Figure 5: Schematic bunch train separation scheme around an interaction point [25].

each of four short trains that could be seen as a single bunch by the detectors. The length of each train $\sim 100\,\mathrm{m} \ll C/4$.

Bunches were separated at the new parasitic encounters near each interaction point by local vertical bumps on either side of the interaction point (Figure 5). It remained possible to separate at the interaction point for injection and ramping. Unlike CESR's very different bunch-train scheme, there was nominally no crossing angle at the interaction point.

LEP was operated with $4 \times 3$ bunches at Z energy in 1995 and with $4 \times 2$ bunches for short periods in 1996–97 at $E = 65$–$70\,\mathrm{GeV}$. Trains of 4 bunches were never used in operation.

### 4.3.1 Side effects

At first sight, the bunch train scheme looks simpler than the pretzel scheme in that the optics differ only in a small, non-dispersive fraction of the ring. Some vertical dispersion was generated by the bumps themselves of course, but this could be minimised by choosing the polarities of the bumps. However the most complicated and pernicious effects arose from the parasitic beam-beam kicks in trains of 3 or 4 bunches.

Different bunches in a train saw a different sequence of beam-beam kicks. Thus each could have different orbits, optics, tunes and even separations at the interaction points. It was not possible to steer out residual vertical separations (which were a significant fraction of the beam size) for all pairs of colliding bunches at the same time [24]. Operation with 4 bunches per train was ruled out. With 3 bunches per train,

these effects reduced the beam-beam strength parameter and specific luminosity [25]. Thus, despite increasing the current by 50% with $k_b = 12$ the peak luminosity eventually achieved at Z energy was the same as previously.

Good beam-beam performance was obtained at 65 GeV by going back to $k_b = 8$ with 2 bunches per train, restoring symmetry of parasitic beam-beam effects between bunches.

From a technical point of view, the development of a self-consistent multi-bunch closed orbit and optics calculation [26], including the beam-beam kicks, for the system of $2 \times 4 \times (4, 3, 2)$ bunches is noteworthy.

#### 4.3.2 MONOCHROMATIZATION AND COLLISION ENERGY SHIFT

Monochromatization of the collision energy is a goal for the $\tau$-charm Factory but actually happened to a small extent in LEP's bunch train scheme. Since it was of electrostatic origin, the dispersion created at the IP in the bunch train scheme had a component with opposite sign for the two beams $D_y^+ - D_y^- \neq 0$. The resulting anti-correlation of energy deviation and vertical position in the two beams can modify the energy spread in collision in the well known way [27].

An additional effect related to monochromatization [30] is the shift in the mean centre-of-mass energy of collisions when the pairs of colliding bunches also have a small *separation*, $y^+ - y^- \neq 0$, at the IP

$$\frac{\Delta w}{E_0} = -\frac{(y^+ - y^-)(D_y^+ - D_y^-)}{2\sigma_y^{*2}}\sigma_\varepsilon^2 \tag{11}$$

Normally this can be steered out by adjusting the separators. However since the dispersions and orbits could vary from bunch to bunch in a train, this was not possible in general for the bunch train scheme.

This shift could have values of several MeV and differ among four experiments and was a potential problem in LEP where the energy must be known with high precision. It was controlled by overlap optimisation in separator scans [28].

### 4.4 General remarks on multi-bunch schemes

I think that the LEP experience with multi-bunch schemes holds some general lessons for future $\mathrm{e^+e^-}$ factories. To gain luminosity, it is clearly not enough to increase the number of bunches: the current per bunch and the effective beam-beam parameter, $\xi_y$ have to be maintained. If new instability mechanisms manage to reduce the beam current by any more than a factor $\sqrt{k_b^{\mathrm{old}}/k_b^{\mathrm{new}}}$ then there will be no gain in performance.

To maintain $\xi_y$, a first step is to correct the optical side effects that tend to shift the orbits and optics of the beams. Since straightforward static corrections act on each bunch of one beam in the same way, it is extremely important to avoid effects that can lead to different bunches in the same beam having different orbits and optical functions. Such effects are very difficult to control.

# 5 LEP2

With the continual addition of super-conducting RF cavities, LEP's energy rose above the W-pair threshold $w = 161\,\mathrm{GeV}$ in 1996 and has now reached 91.5 GeV per beam. Further steps in energy will be taken in the next few years.

## 5.1 Attaining high luminosity

As at LEP1, beam size controls are an essential tool for maximising luminosity. However at LEP2 energies, the radiation from wigglers is too intense and variation of $J_x$ is the only practical method for adjusting the horizontal emittance $\epsilon_x$ in a given optics. This control came into regular operational use this year.

| | | | |
|---|---|---|---|
| Beam energy | $E$ | 91.5 | GeV |
| No. of bunches | $k_b$ | 4 | |
| Damping partition | $J_x$ | 1.6 | |
| | $J_y$ | 1 | |
| | $J_\epsilon$ | 1.4 | |
| Main bend field | $B_0$ | 0.101 | T |
| Field in emittance wigglers | $B_{\mathrm{EW}}$ | 0 | T |
| Critical energy of syn. radn. | $u_c$ | 562 | keV |
| Photon emission rate | $N/c$ | 0.62 | photons/m |
| Energy loss/turn | $U_0$ | 2049 | MeV |
| Radial damping time | $\tau_x$ | .005 | s |
| | $\tau_x/T_0$ | 56 | turns |
| Energy spread | $\sigma_\varepsilon$ | $1.72 \times 10^{-3}$ | |
| Emittances (no beam-beam) | $\epsilon_x$ | 30 | nm |
| | $\epsilon_y$ | .26 | nm |
| Particles/bunch | $N_b$ | $2.78 \times 10^{11}$ | |
| Single bunch current | $I_b$ | 0.5 | mA |
| Twiss functions at interaction point | $\beta_x^*, \beta_y^*$ | 1.5,0.05 | |
| Beam sizes at interaction point | $\sigma_x^*, \sigma_y^*$ | 211,3.6 | $\mu$m |
| Radiated power (2 beams) | $P_{\mathrm{rad}}$ | 8.2 | MW |
| Beam-beam parameters | $\xi_x, \xi_y$ | .023,.05 | |
| Luminosity | $L$ | $4 \times 10^{31}$ | $\mathrm{cm}^{-2}\mathrm{s}^{-1}$ |
| Peak RF voltage | $V_{\mathrm{RF}}$ | 2345 | MV |
| Synchrotron tune | $Q_s$ | 0.107 | |
| Bunch length (low current) | $\sigma_z$ | 1.26 | cm |
| Beam-beam lifetime | $\tau_b b$ | 6.2 | h |

Table 3: A calculated set of parameters consistent with good performance achieved in recent operation in 1997.

Figure 6 shows the accessible range of horizontal emittance, $\epsilon_x$ as a function of energy for the standard $(90^\circ, 60^\circ)$ optics. Some principal operating ranges (LEP1, LEP1.5, LEP96, LEP97) are indicated. The quadratic curves show the natural variation of $\epsilon_x \propto E^2/J_x$ for typical values of $J_x \geq 1$. An additional curve shows the maximum $\epsilon_x$ attainable with the emittance wigglers and the nominal $J_x = 1$. The upper limit to $\epsilon_x$, set by the dynamic aperture (see later), could in principle be reached with $J_x < 1$ and the wigglers. The corresponding curves in Figure 7 show the *maximum* current consistent with the beam-beam limit in both planes according to (6) and a model of the beam-beam blow-up in which the maximum $\xi_y$ attainable varies slowly from 0.048 at 46 GeV to 0.053 at 100 GeV. However experience at LEP [10] strongly suggests that $\xi_x$ is limited at a value lower than $\xi_y$, perhaps $\xi_x \simeq 0.04$. Provided $\sigma_y^*$ can be made small enough though, (6)-(8) show that high luminosity with high $\xi_y$ remains possible. Thus the luminosity already exceeds what might be expected for a given $\epsilon_x$ thanks to the operators' prowess in reducing $\sigma_y^*$.

For high values of $\xi_y$, reducing the value of $\beta_x^*$ may help to avoid the horizontal beam-beam limit; $\beta_x^*$ has recently been reduced from 2.5 m to 1.5 m.

Table 3 is a set of parameters consistent with recently achieved high luminosity conditions.

### 5.2 Vertical beam size

Reduction of the vertical beam size is the royal road to luminosity. Figure 9 shows the vertical emittance inferred from scans of the vertical separation at the interaction points as a function of the fill number in 1997. As time goes on, the tuning of the machine is improved to the point where $\sigma_y^*$ comes down dramatically and performance really takes off. This behaviour is typical of what has happened since 1994 when the golden-orbit procedure was established. The time taken from a machine start-up (following a shutdown or major change) to obtain small beam size has also come down since then. Now it is typically a week or two.

Simulations of the vertical beam size in ensembles of imperfect machines, corrected according to procedures similar to those used in the control room, are in good quantitative agreement: compare Figure 10 with Figure 9. There is a strong correlation with the residual vertical dispersion after the orbit and optics are corrected.

Frequent fine-scans ("Vernier") of the vertical separation at the interaction points are now a standard operational procedure. The luminosity variation provides a good measurement of vertical beam size (translated into emittance in Figure 9).

### 5.3 Single particle dynamics with radiation

The huge radiation energy loss of about 2 % per turn, replaced by RF cavities in discrete locations, produces the "energy sawtoothing" effect shown in Figure 11. Since the electron beam has almost exactly equal and opposite momentum deviation, *yet must be focused by the same magnets*, there are dramatic effects on the orbit and lin-

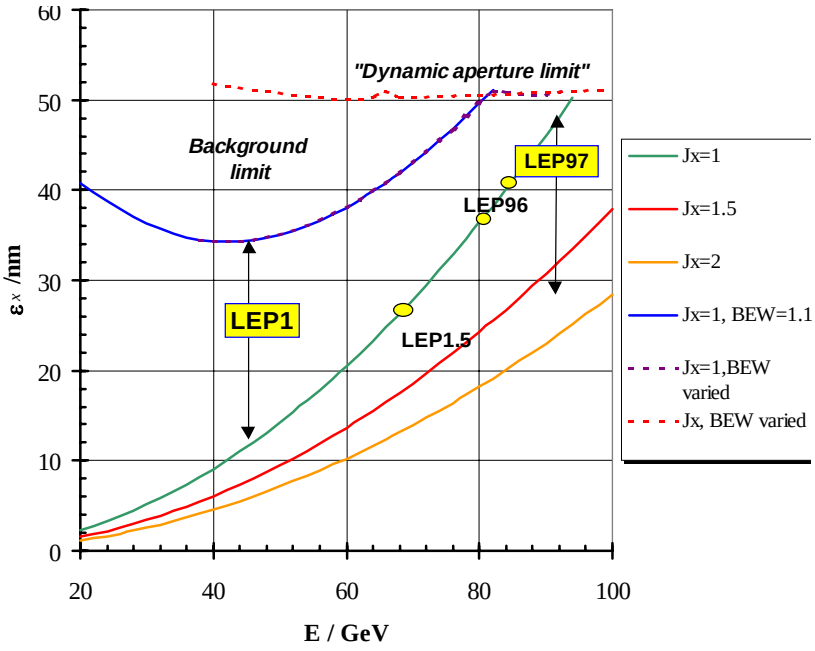


Figure 6: Horizontal emittance range for the $(90°, 60°)$ optics.

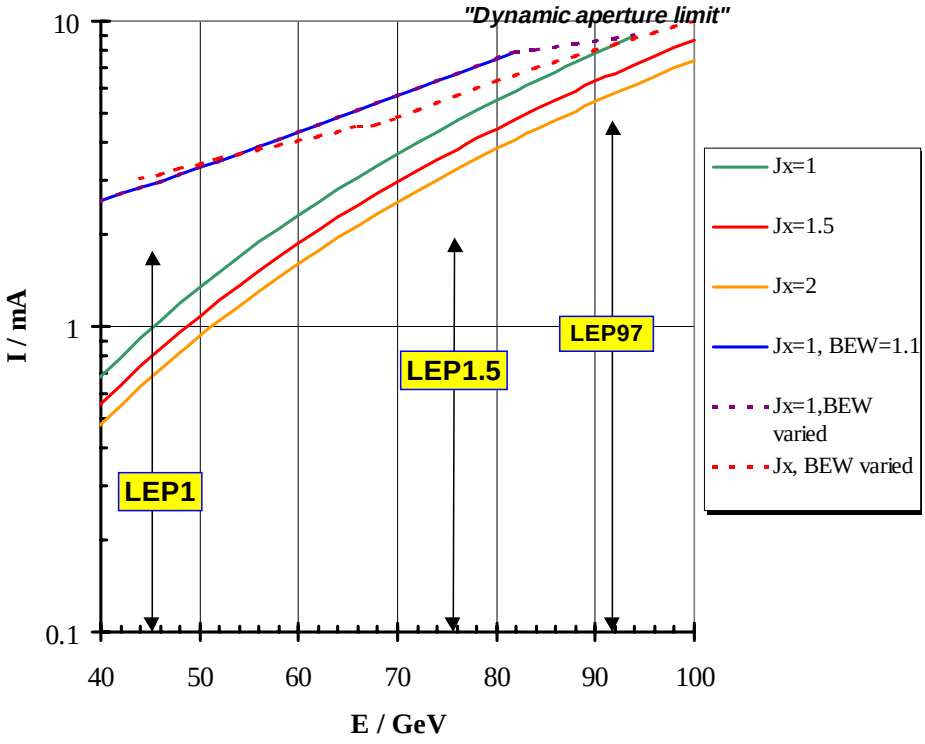


Figure 7: Maximum single-beam current ($k_b = 4$) at the beam-beam limit.

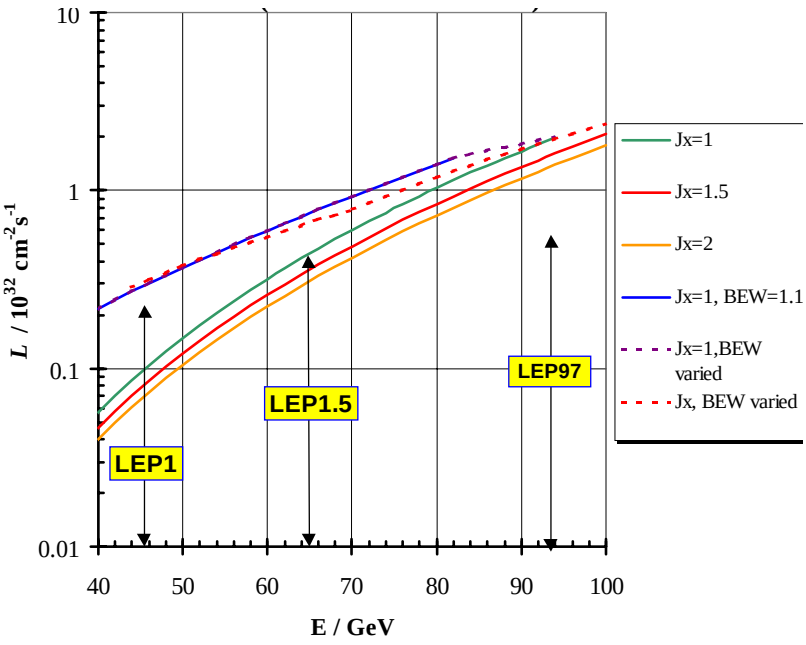


Figure 8: Luminosity for $(90°, 60°)$ at beam-beam limit with unlimited beam current.

ear optics. Quadrupoles have different focusing strength when particles have different momentum so the energy differences translate into local differences in orbits, phase advances and optical functions. The RF cavities have to be thought of as an essential part of the linear optics. Figures 12–14 provide some illustration of the magnitude of these differences.

I do not have time to present the formalism necessary for a full analysis. Clearly the usual "Courant-Snyder" formulation of linear optics, treating the transverse and longitudinal motions on a very different footing, is quite inadequate for LEP2.[5] The variation of momentum on the closed orbit in 6D phase space is much larger than the typical magnitude of synchrotron oscillations around it. A full 6D formulation of beam optics is necessary, in terms of the eigenvectors of linear motion around the closed orbit; the essence of this can be found in [31]. To generalise intuitions related to $\beta$-functions and phases, it is helpful to introduce the nine Mais-Ripken [32] functions

$$\begin{pmatrix} \beta_{x1} & \beta_{x2} & \beta_{x3} \\ \beta_{y1} & \beta_{y2} & \beta_{y3} \\ \beta_{z1} & \beta_{z2} & \beta_{z3} \end{pmatrix} \tag{12}$$

and the phases $(\mu_1, \mu_2, \mu_3)$ of the normal modes. In this formalism the dispersion functions appear on a more symmetric footing as amplitude functions for the projection

[5] Although unphysical, it is of some use as a technical tool in optics design.

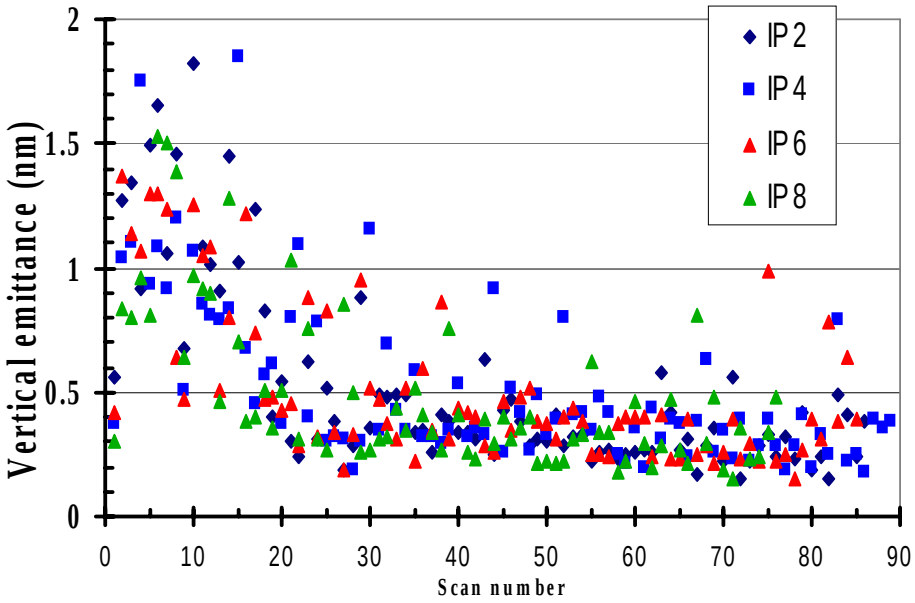


Figure 9: The vertical emittance inferred from separator scans. Data from 1997 run at 91.5 GeV per beam (courtesy M. Lamont).

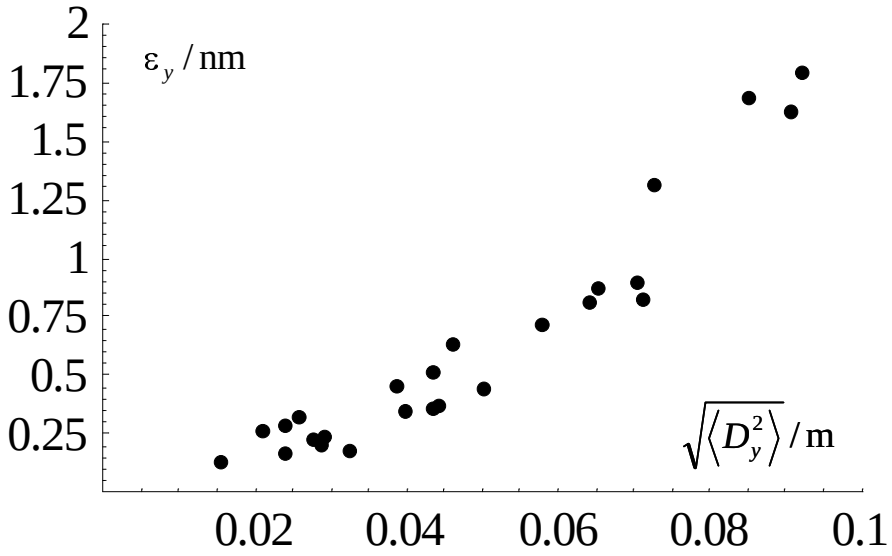


Figure 10: Vertical emittance found by simulation in an ensemble of corrected imperfect machines $(90°, 60°)$ vs. RMS vertical dispersion

of the synchrotron mode into the transverse planes:

$$D_x = \sqrt{\frac{\beta_{x3}}{\gamma_{t3}}} \cos\left(\mu_3 + \phi\right). \tag{13}$$

These formalisms are fully implemented in the program MAD [33] and we use them regularly to compute the optical effects of radiation and RF.

### 5.4 Nonlinear Dynamics and Dynamic Aperture

In general, agreement between the computed and measured dynamic apertures of LEP is very good, provided sufficient effort is put into modelling the particle dynamics, the machine imperfections and the way in which the operators correct them.

The strong radiation effects play an important role in the nonlinear dynamics at large amplitudes, to the extent that the dynamic aperture problem for LEP is quite different from most other colliders. The rapid radiation damping (Table 3) means that, for LEP2, 100 turns is "long-term tracking" and that quadrupoles are nonlinear optical elements (because the energy lost in a quadrupole is $\propto K_1^2(x^2+y^2)$).

The energy lost in quadrupoles is responsible for the ultimate limit of the dynamic aperture. At large betatron amplitudes, the additional energy lost is so much that particles want, so to speak, to oscillate about a different "stable phase angle" in longitudinal phase space. Large amplitude betatron motion generates a peculiar kind of synchrotron motion. Eventually the RF voltage available is not enough to focus these particles and they are lost. This rough description needs to be made more precise, especially given the small ratio ($\simeq 5$) of the damping time to the synchrotron period. The typical behaviour is most readily understood from tracking results [34, 35]. In fact, this radiative beta-synchrotron coupling (RBSC) effect rarely occurs in isolation but usually acts to enhance other effects, such as nonlinear resonances, that initiate an amplitude growth.

As the biggest contribution to RBSC comes from the low-$\beta$ quadrupoles, this effect can also be a limit to the strength of focusing at the interaction point, quite independent of the usual chromatic effects of the insertions.

Most often, however, some other effect limits the dynamic aperture before the RBSC limit is reached. In the standard lattice with $(\mu_x, \mu_y) = (90^\circ, 60^\circ)$, for example, the horizontal dynamic aperture is limited by a rather strong shift of the vertical tune with the horizontal action variable, $\partial Q_y/\partial I_x < 0$, bringing $Q_y$ down onto the integer. For some years we worried that the resulting dynamic aperture would not be enough to accomodate the large $\epsilon_x \propto E^2$ at high energy. However this all hinged on having some criterion for how many beam $\sigma$s would need to fit inside the dynamic aperture. Experience with this optics up to the present energies has shown that, because the motion stays rather linear most of the way out to the dynamic aperture, the conventional "$10\sigma$ with $J_x = 1$" criterion was rather conservative and about $7\sigma$ seems to be ample *(for this optics)*. Coupled with the increase in $J_x$ that is necessary anyway, this means that we can, after all, operate this optics for physics at the highest energies the RF system will allow.

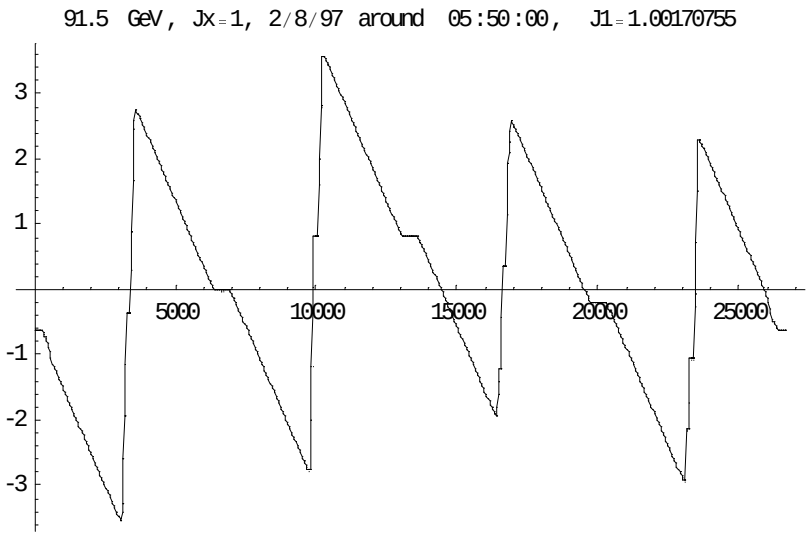


Figure 11: Variation of the fractional momentum deviation (in units of $10^{-3}$) versus $s$ from nominal on the closed orbit of 92 GeV positrons (moving from left to right). The distribution of RF voltage in relation to the smooth energy loss by synchrotron radiation in the arcs of the ring is imprinted on the pattern. The whole circumference of LEP is shown.

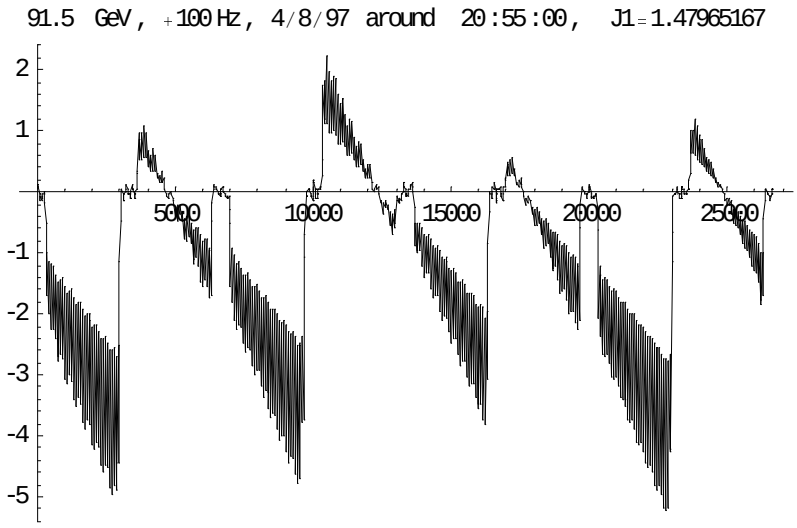


Figure 12: Horizontal closed orbit of positrons (in mm) versus $s$ showing the effect of increasing the RF frequency to move the orbit inwards. This increases $J_x$ to about 1.5 and reduces $\epsilon_x$. The electron orbit is roughly (but not exactly! [29]) equal and opposite. Even allowing for machine imperfections, residual separations at the interaction points remain small.

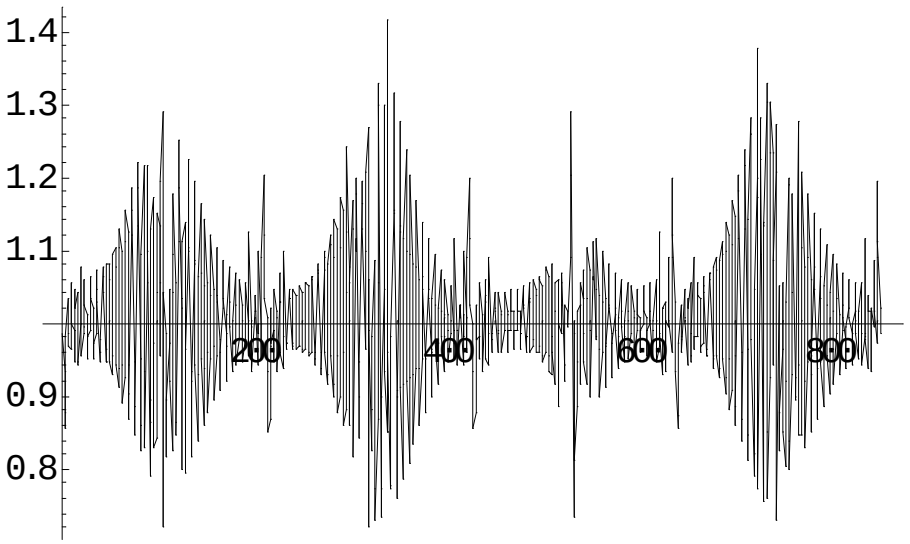


Figure 13: Ratio of the Mais-Ripken function $\beta_{y2}$, including the effects of RF and radiation, to the Courant-Snyder function $\beta_y$, computed for 1 92 GeV $e^+$ beam in an ideal LEP.

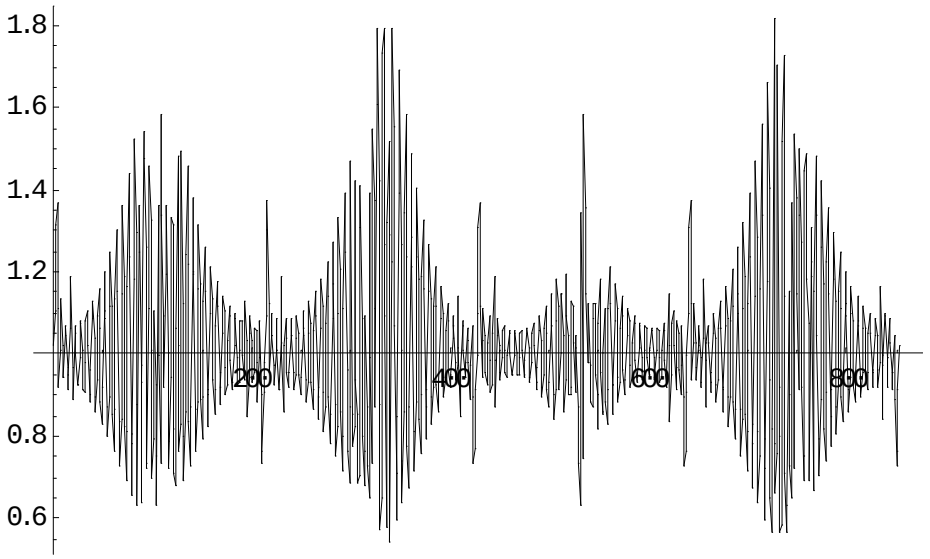


Figure 14: Ratio of the Mais-Ripken functions for positrons and electrons, $\beta^+_{y2}/\beta^-_{y2}$. This is the same case as Figure 13 and shows how different the optics of two beams in the same ring can be.

Nevertheless, we are still interested in running LEP with higher values of $\mu_x$. The advantage is not so much the lower emittance, $\epsilon_x$, though that is useful, but the lower momentum compaction $\alpha_c \propto \mu_x^{-2}$ which would allow higher energy for a given $V_{\rm RF}$. Increasing $J_x$ is an easier way to reduce $\epsilon_x$ and gain luminosity (at the price of a little more $V_{\rm RF}$).

It is well known that $\mu_x = 135^\circ$ gives the minimum emittance for a FODO lattice. However it was hard to get a circulating beam with this choice because of the large horizontal detuning, $\partial Q_x/\partial I_x < 0$ (recall that $\partial Q_x/\partial I_x$ becomes very large as $\mu_x \to 2\pi/3^{\mp}$) [36, 35].

Moving to $\mu_x = 3\pi/5 = 108^\circ$ (and keeping $\mu_y = \pi/2$) reduces $\partial Q_x/\partial I_x$ to a tolerable positive value and the dynamic aperture was predicted to be large, limited by numerous imperfection-driven resonances combining with RBSC. With the typical tune $Q_x(0) \simeq 102.27$, particles are brought onto the resonance $3Q_x = 307$ at amplitudes within the dynamic aperture. The damping and detuning are large enough that the resonance does not directly cause instability. This was confirmed by dynamic aperture measurements (by the kicked-beam method) which gave values, as usual, within 10% or so of those found by tracking with radiation damping [36, 35]. Measurements of the loss following a kick had a feature showing the resonance amplitude and it also manifests itself in the motion of the centre of gravity of the beam following a kick [39].

It turned out that the resonance structure at large amplitudes modifies the transport mechanisms determining the beam tails and may actually reduce the beam lifetime in cases when $\epsilon_x$ was made sufficiently large. Beam tail measurements [37] were very useful here.

While an operational test has shown that there is still plenty of margin for this optics to operate up to 100 GeV (provided very large emittances are avoided), another optics [38], with $\mu_x = 17\pi/30$ and smaller $\partial Q_x/\partial I_x$, will be tried out very soon. Although its energy reach is a little less, it may be more comfortable to operate.

# 6 Conclusions

The flexibility built into the basic design of LEP has allowed its performance to be maximised in a wide range of operating conditions. It is better to design an $\rm e^+e^-$ collider optics with a relatively *low emittance* and provide the capability to increase it in a controlled way as the stored beam current increases.

Schemes to allow larger numbers of bunches may introduce unwanted side-effects. Expected gains in luminosity will come only if they can be corrected. *Differences between bunches in the same beam,* the progeny of parasitic beam-beam encounters, are among the most difficult effects to compensate. On the other hand, the LEP experience shows that you *can* get high performance by colliding *two beams with very different optics and orbits* in the same ring.

Beam dynamics at LEP2 has many novel features because of the strong synchrotron radiation effects.

**Further information**

The list of references below is a tiny sample of the literature on LEP: the proceedings of recent accelerator conferences contain many more. The LEP Performance Workshops [40] are a useful source of detail on developments since LEP was commissioned. The transparencies of this talk, with additional figures and other material (in colour) are available at [1].

**Acknowledgement:**

Needless to say, I have drawn on the work of many people (including about a third of this audience!) involved in the LEP project over the last 20 years or so.

## References

[1] `http://wwwslap.cern.ch/~jowett/icfa/frascati97/LEP/`

[2] S. Myers, "A Possible New Injection and Accumulation Scheme for LEP", CERN LEP Note 334, 1981.

[3] P. Baudrenghien, P. Collier "Double Batch Injection into LEP", Proc. European Particle Accelerator Conference, Barcelona 1996, IOP, (1996) 415.

[4] A. Hutton et al, "Improvements to the LEP Lattice Design", Proc. 12th Int. Conf. on High-Energy Accelerators, Fermilab (1983) 164.

[5] LEP Design Report, Vol. II, The LEP Main Ring, CERN-LEP/84-01 (1984).

[6] J.M. Jowett, T.M. Taylor, "Wigglers for Control of Beam Characteristics in LEP", IEEE Trans. Nucl. Sci. **30** (1983) 2581.

[7] A. Blondel and J.M. Jowett, "Wigglers for polarization", in "Polarization at LEP", in G. Altarelli et al. (Eds.), CERN 88-06 (1988).

[8] J.M. Jowett "Introductory Statistical Mechanics for Electron Storage Rings", in M. Month and M. Dienes (Eds.), "Physics of Particle Accelerators", AIP Conf. Proc. 153 (1987) 864.

[9] P.Collier, H. Schmickler, Proc. Particle Accelerator Conference 1995, 545.

[10] H. Burkhardt, these proceedings.

[11] M. Placidi and J. Wenninger, these proceedings.

[12] B. Zotter, "Comparison of Theory and Experiment on Beam Impedance: the Case of LEP", Proc. European Particle Accelerator Conference 1992, 273.

[13] D. Brandt et al, Proc. 1993 Particle Accelerator Conf., IEEE, Proc. Particle Accelerator Conference 1993, (1993) 3429.

[14] D. Brandt et al, Proc. Particle Accelerator Conference 1995, 570.

[15] P. Collier et al, Proc. European Particle Accelerator Conference 1996, 418.

[16] See 2+2 particle model in: K. Cornelis, M.Lamont, “Head-tail instabilities enhanced by the beam-beam interaction”, Proc. European Particle Accelerator Conference 1994, 1150 and and simulation in: G. Li, K. Cornelis, CERN SL/94-85.

[17] E. Keil, CERN LEP/70-7 (1977).

[18] J.T. Rogers, these proceedings.

[19] C. Rubbia, “The ‘future’ in high-energy physics’, Proc. European Particle Accelerator Conference1988, 290.

[20] J.M. Jowett, “More bunches in LEP”, Proc. Particle Accelerator Conference, Chicago, 1989, 1806.

[21] “Report of the Working Group on High Luminosities at LEP”, E. Blucher, J.M. Jowett, F. Merritt, G. Mikenberg, J. Panman, F. Renard, D. Treille (Eds.), CERN Report, 91-02 (1991). E. Blucher et al, CERN 91–02 (1991).

[22] L. Arnaudon et al, CERN SL-MD Note 150 (1994).

[23] E. Keil, in Lecture Notes in Physics **425**, Springer (1994) 106.

[24] O. Brunner et al, Proc. Particle Accelerator Conference, Dallas 1995, 514.

[25] P. Collier et al, Proc. European Particle Accelerator Conference’96 876.

[26] E. Keil, “Truly self-consistent Treatment of the Side Effects with Bunch Trains”, CERN SL/95-75 (1995).

[27] See J.M. Jowett, in [23] for a review.

[28] M. Böge et al, Proc. European Particle Accelerator Conference 1996, 427.

[29] M. Bassetti, “Effects due to the discontinuous replacements of radiated energy in an electron storage ring”, Proc. XIth International Conference on High-Energy Accelerators, Geneva 1980, Birkhäuser, Basel, 1981.

[30] J.M. Jowett et al, CERN SL-Note 95-46 (OP) (1995).

[31] A. Chao, “Evaluation of beam distribution parameters in an electron storage ring”, Journal of Applied Physics **50** 595-598, 1979.

[32] H. Mais and G. Ripken, “Theory of Coupled Synchro-Betatron Oscillations”, DESY internal Report, DESY M-82-05, 1982.

[33] H. Grote, F.C. Iselin, “The MAD program (methodical accelerator design) ; user’s reference manual”, CERN SL 90–13 (AP) rev. 5 (1996).

[34] F. Barbarin, F.C. Iselin, and J.M. Jowett, “Particle dynamics in LEP at Very High Energy”, Proceedings of the Fourth European Particle Accelerator Conference, Proc. European Particle Accelerator Conference 1994, World Scientific, Singapore, 1994, p. 193.

[35] Y. Alexahin et al, “The Dynamic Aperture of LEP at High Energy”, EPAC’96, Sitges, June 1996.

[36] Y. Alexahin, “Improving the dynamic aperture of LEP2”, CERN–SL–95–110 (AP) 1995.

[37] I. Reichel, this workshop.

[38] A. Verdier, CERN internal meetings, unpublished.

[39] J.M. Jowett, “Non-linear resonances: predictions effects and measurements” in Proc. 7th Workshop on LEP Performance [40].

[40] J. Poole (Ed.), Proc. First to Eighth Workshops on LEP Performance, Chamonix (WLP), CERN SL/91-23 (1991), SL/92-29 (1992), SL/93-19 (1993), CERN SL/94-06 (1994), CERN SL/95-08 (1995), CERN SL/96-05 (1996), CERN SL/97-06 (1997), CERN SL/98-006 (1998) and

`http://www.cern.ch/CERN/Divisions/SL/news/news.html`